Generation of six-partite continuous-variable entanglement using a nonlinear photonic crystal by frequency conversions

Yi Gu,[1] Guangqiang He,[1,*] and Xufei Wu[1,2]

[1]*State Key Laboratory of Advanced Optical Communication Systems and Networks, Department of Electronic Engineering, Shanghai Jiao Tong University, Shanghai 200230, China*

[2]*Department of Physics, Shanghai Jiao Tong University, Shanghai 200230, China*

(Received 5 January 2012; published 29 May 2012)

We theoretically show that six-partite continuous-variable entanglement can be generated by nonlinear optical processes conducted in a designed photonic crystal-like periodically poled lithium niobat (PPLN). The processes consist of a nonlinear parametric down-conversion and four sum-frequency processes. The characteristics of the six-partite entanglement among the six beams are analyzed both above and below the threshold by applying a sufficient inseparability criterion for multipartite continuous-variable entanglement. We investigated our proposal for a specific case of a PPLN optical superlattice with fixed light and material properties.

DOI: 10.1103/PhysRevA.85.052328 PACS number(s): 03.67.Bg, 03.67.Mn, 42.50.Dv

I. INTRODUCTION

Entanglement is a mysterious and important quantum phenomenon. In addition, entanglement is the fundamental resource of quantum communication and quantum computation [1], so the generation of quantum entanglement is attractive, and a lot of research is focused on this promising area. Originally, the most effort was devoted to discrete-variable entanglement [2,3]. Recently, continuous-variable (CV) entanglement is raising more concern because of its high efficiency [4]. Particularly, multipartite CV entanglement is a crucial resource of multipartite quantum communication [5–8]. As a result, theoretical studies have been conducted focusing on the generation of CV multipartite entanglement [9–11]; in addition, some experimental studies have also been conducted [5,12–14]. The generation of tripartite CV entanglement [9,12,14] and quadripartite CV entanglement [10,11,13] has been studied. The sufficient inseparability criterion for CV multipartite entanglement is proposed by van Loock and Furusawa [15], and the characteristics of the generated entanglement can be investigated by employing this criterion. Until now, two methods have been employed to generate CV multipartite entanglement. One is to generate entanglement by mixing squeezed beams on unbalanced beam splitters [5,14], but the limit of this method is that only entanglement among modes with the same frequency can be generated. The other method is to generate multipartite entanglement by nonlinear optical processes, and nonlinear optical processes can be realized using nonlinear photonic crystals [16].

In Leng *et al.*'s important and inspiring work [11], quadripartite entanglement is generated by down-conversion cascaded with sum frequencies; however, the entanglement characteristics when the pump is above the threshold is not discussed in that work. We not only extended Leng *et al.*'s proposal to generate six-partite entanglement but also investigated the entanglement characteristics both below and above the threshold. In our research, we generate CV genuine six-partite entanglement by a nonlinear intracavity down-conversion cascaded with four sum-frequency processes. After the first two beams are generated by a parametric down-conversion in the superlattice, the third beam is generated by a double sum frequency of the pump and the first beam, the fourth beam is generated by a similar sum frequency of the pump and the second beam, the fifth beam is generated by the pump and the third beam, and finally, the sixth beam is generated by the pump and the fourth beam. Compared to other methods to generate multicolor entanglement [10,13], our proposal has an advantage. For instance, compared to Pysher *et al.*'s work [13], the advantage of our proposal is that the crystal used for nonlinear processes can be designed flexibly to improve the efficiency. And the crystal can be designed to fulfill more nonlinear processes so that more entangled modes can be generated.

This paper is arranged as follows. In Sec. II, the physical model and the experiment setup for the generation of CV six-partite entanglement are introduced and discussed. In Sec. III, the threshold is investigated and the mean values and fluctuations of the output fields are derived. In Sec. IV, the entanglement characteristics of the six nonpump modes are investigated. Finally, some conclusions are drawn.

II. CASCADED NONLINEAR PARAMETRIC PROCESSES

In this work, six output modes are generated by a pump with frequency ω_0 in an optical oscillator cavity. The six modes are generated by a down-conversion and four sum-frequency processes. The experiment setup for the system is depicted in Fig. 1. A pump beam is injected into an optical oscillator cavity generating six beams with different frequencies. Then the output of the six beams with frequency ω_i $(i = 1, \ldots, 6)$ from another mirror are separated by a triangular prism. The separated beams are analyzed by the Fabry-Pérot (FP) analysis cavities, similar to Coelho *et al.*'s method [12]. The output beam with frequency ω_0 from the left mirror is reflected by the polarizing beam splitter (PBS) and enters the FP analysis cavity. The nonlinear processes are conducted using a periodically poled lithium niobat (PPLN) optical superlattice (OS). The sketch of the optical oscillator including the OS is plotted in Fig. 2. We will describe the generation of the

*Corresponding author. gqhe@sjtu.edu.cn

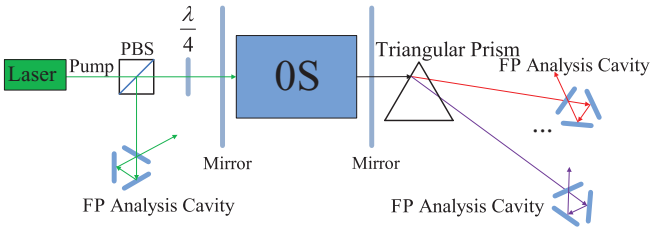

FIG. 1. (Color online) The scheme of the experiment setup. PBS, polarizing beam splitter; $\lambda/4$, quarter-wave plate; OS, optical superlattice; FP analysis cavity, Fabry-Pérot analysis cavity. The green beam (left) is the pump beam, and the red beam and the purple beam (right) are the output beams with frequencies ω_2, which is the smallest, and ω_5, which is the largest, respectively; other beams and their individual FP analysis cavities are replaced by ellipsis since they are similar.

six modes in five steps. First, two beams with frequency ω_1 and ω_2 are generated by a down-conversion of the pump (PDC). Second, the third beam with frequency ω_3 is generated by a sum frequency of the pump with frequency ω_0 and the first beam with frequency ω_1 (SFG1). Third, the fourth beam with frequency ω_4 is generated by a sum frequency of the pump with frequency ω_0 and the second beam with frequency ω_2 (SFG2). Fourth, the fifth beam is generated by a sum frequency of the pump with frequency ω_0 and the third beam with frequency ω_3 (SFG3). Last, the sixth beam is generated by a similar sum frequency of the pump with frequency ω_0 and the fourth beam with frequency ω_4 (SFG4). In addition, five reciprocals, G_1, G_2, G_3, G_4, G_5, are needed to compensate the phase mismatching of the five nonlinear processes. To obtain the reciprocal-lattice vector for corresponding quasiphase matching, an OS is needed, and the superlattice can be designed using a dual-grid method to obtain better entanglement characteristics [16]. Assuming that the wavelengths of beams with frequency ω_i $(i = 0, \ldots, 6)$ are 532, 900, 1354, 341, 388, 210, and 227 nm, respectively, and temperature is 25°C, the PPLN OS can be designed for nonlinear optical processes. The tiling vectors of the OS are calculated to be 0.264, 0.534, 0.391, 2.27, and 1.79 μm. The structure of the PPLN OS is shown in Fig. 3, where the index of refraction of the black blocks is negative and the index of refraction of the white blocks is positive. The unit of length in Fig. 3 is meters.

The quasiphase-matching sketch for the nonlinear processes is plotted in Fig. 4. The energy conversion and

FIG. 3. The structure of the PPLN OS.

phase-matching conditions can be written as follows:

$$\begin{aligned}
&\text{PDC: } \omega_0 = \omega_1 + \omega_2, k_0 = k_1 + k_2 + G_1,\\
&\text{SFG1: } \omega_3 = \omega_0 + \omega_1, k_3 = k_0 + k_1 + G_2,\\
&\text{SFG2: } \omega_4 = \omega_0 + \omega_2, k_4 = k_0 + k_2 + G_3,\\
&\text{SFG3: } \omega_5 = \omega_0 + \omega_3, k_5 = k_0 + k_3 + G_4,\\
&\text{SFG4: } \omega_6 = \omega_0 + \omega_4, k_6 = k_0 + k_4 + G_5.
\end{aligned} \tag{1}$$

III. CALCULATION OF OUTPUT FIELDS

According to the nonlinear processes proposed above, the interaction Hamiltonian H_I for the cascaded nonlinear processes, the Hamiltonian for the pump beam H_p, and the damping term of ith mode in cavity L_i read as follows [17]:

$$\begin{aligned}
H_I = {} & i\hbar(\kappa_1 \hat{a}_0 \hat{a}_1^\dagger \hat{a}_2^\dagger + \kappa_2 \hat{a}_0 \hat{a}_1 \hat{a}_3^\dagger \\
& + \kappa_3 \hat{a}_0 \hat{a}_2 \hat{a}_4^\dagger + \kappa_4 \hat{a}_0 \hat{a}_3 \hat{a}_5^\dagger + \kappa_5 \hat{a}_0 \hat{a}_4 \hat{a}_6^\dagger) + \text{H.c.},
\end{aligned} \tag{2}$$

$$H_p = i\hbar\varepsilon \hat{a}_0^\dagger + \text{H.c.}, \tag{3}$$

$$L_i \hat{\rho} = \gamma_i [2\hat{a}_i \hat{\rho} \hat{a}_i^\dagger - \hat{a}_i^\dagger \hat{a}_i \hat{\rho} - \hat{\rho} \hat{a}_i^\dagger \hat{a}_i], \tag{4}$$

where κ_i $(i = 1, \ldots, 5)$ are the dimensionless nonlinear coupling coefficients of the five nonlinear processes, $\hat{a}_i$ are annihilation operators of the modes in the cavity with frequency ω_i, γ_i are the damping rates $(i = 0, \ldots, 6)$, ε is the pump amplitude and is set real, and $\hat{\rho}$ is the density matrix of the interested system. The master equation reads [17]

$$\frac{\partial \hat{\rho}}{\partial t} = -\frac{i}{\hbar}[H_p + H_I, \hat{\rho}] + \sum_{i=1}^{5} L_i \hat{\rho}, \tag{5}$$

The above master equation can be converted into the equivalent c-number Fockker-Planck equation in P representation, which may be written as a completely equivalent stochastic differential equation [17]:

$$\tau \frac{\partial}{\partial t} \tilde{\alpha} = F + B\eta, \tag{6}$$

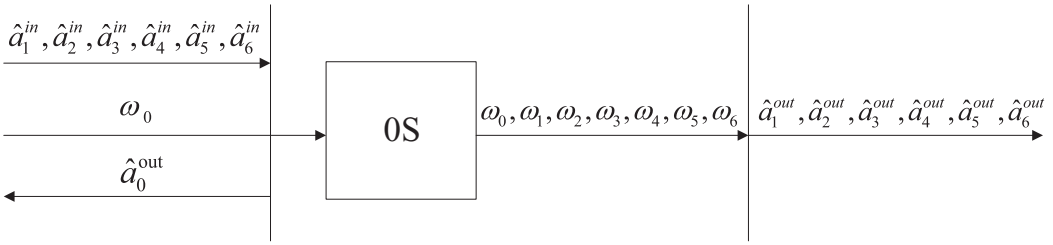

FIG. 2. Sketch of the optical oscillator cavity including OS which is used to provide reciprocals for the nonlinear interactions. Six modes of light fields with frequency ω_1, ω_2, ω_3, ω_4, ω_5, and ω_6 are generated in the cavity driven by a pump field with frequency ω_0. $\hat{a}_i^{in}$ and $\hat{a}_i^{out}$ $(i = 1, \ldots, 6)$ are annihilation operators of the input and output fields of the six modes, respectively.

where

$$\tilde{\alpha} = [\alpha_0,\alpha_1,\alpha_2,\alpha_3,\alpha_4,\alpha_5,\alpha_6,\alpha_0^*,\alpha_1^*,\alpha_2^*,\alpha_3^*,\alpha_4^*,\alpha_5^*,\alpha_6^*], \quad (7)$$

$$\eta = [\eta_1,\eta_2,\eta_3,\eta_4,\eta_5,\eta_6,\eta_7,\eta_8,\eta_9,\eta_{10},\eta_{11},\eta_{12},\eta_{13},\eta_{14}], \quad (8)$$

$$D = BB^T, \quad (9)$$

$$D = \begin{bmatrix} d & 0 \\ 0 & d^\dagger \end{bmatrix}, \qquad F = \begin{bmatrix} f \\ f^* \end{bmatrix}, \quad (10)$$

$$d = \begin{bmatrix} 0 & -\kappa_2\alpha_3 & -\kappa_3\alpha_4 & -\kappa_4\alpha_5 & -\kappa_5\alpha_6 & 0 & 0 \\ -\kappa_2\alpha_3 & 0 & \kappa_1\alpha_0 & 0 & 0 & 0 & 0 \\ -\kappa_3\alpha_4 & \kappa_1\alpha_0 & 0 & 0 & 0 & 0 & 0 \\ -\kappa_4\alpha_5 & 0 & 0 & 0 & 0 & 0 & 0 \\ -\kappa_5\alpha_6 & 0 & 0 & 0 & 0 & 0 & 0 \\ 0 & 0 & 0 & 0 & 0 & 0 & 0 \\ 0 & 0 & 0 & 0 & 0 & 0 & 0 \end{bmatrix}, \quad (11)$$

$$f = \begin{bmatrix} \frac{\gamma_0}{2}(\varepsilon-\alpha_0) - \kappa_1\alpha_1\alpha_2 - \kappa_2\alpha_1^*\alpha_3 - \kappa_3\alpha_2^*\alpha_4 - \kappa_4\alpha_3^*\alpha_5 - \kappa_5\alpha_4^*\alpha_6 \\ -\frac{\gamma_1}{2}\alpha_1 + \kappa_1\alpha_0\alpha_2^* - \kappa_2\alpha_0^*\alpha_3 \\ -\frac{\gamma_2}{2}\alpha_2 + \kappa_1\alpha_0\alpha_1^* - \kappa_3\alpha_0^*\alpha_4 \\ -\frac{\gamma_3}{2}\alpha_3 + \kappa_2\alpha_0\alpha_1 - \kappa_4\alpha_0^*\alpha_5 \\ -\frac{\gamma_4}{2}\alpha_4 + \kappa_3\alpha_0\alpha_2 - \kappa_5\alpha_0^*\alpha_6 \\ -\frac{\gamma_5}{2}\alpha_5 + \kappa_4\alpha_0\alpha_3 \\ -\frac{\gamma_6}{2}\alpha_6 + \kappa_5\alpha_0\alpha_4 \end{bmatrix}, \quad (12)$$

where τ is the round-trip time of the light in the cavity and is assumed to be the same for the six modes and the pump field. $\alpha_i = \bar{\alpha}_i + \delta\alpha_i$, where α_i are the fields in the cavity with frequency ω_i, $\bar{\alpha}_i$ are mean values of α_i, and $\delta\alpha_i$ are fluctuations of the fields. η_i ($i = 1,\ldots,14$) are the real noise terms. In order to obtain the steady-state solutions of the above processes, the noise terms and all the fluctuations can be neglected; thus the equations for the mean values of the fields in the cavity can be written as

$$\tau\frac{d\bar{\alpha}_0}{dt} = \frac{\gamma_0}{2}(\varepsilon-\bar{\alpha}_0) - \kappa_1\bar{\alpha}_1\bar{\alpha}_2 - \kappa_2\bar{\alpha}_1^*\bar{\alpha}_3 - \kappa_3\bar{\alpha}_2^*\bar{\alpha}_4 - \kappa_4\bar{\alpha}_3^*\bar{\alpha}_5 - \kappa_5\bar{\alpha}_4^*\bar{\alpha}_6, \quad (13)$$

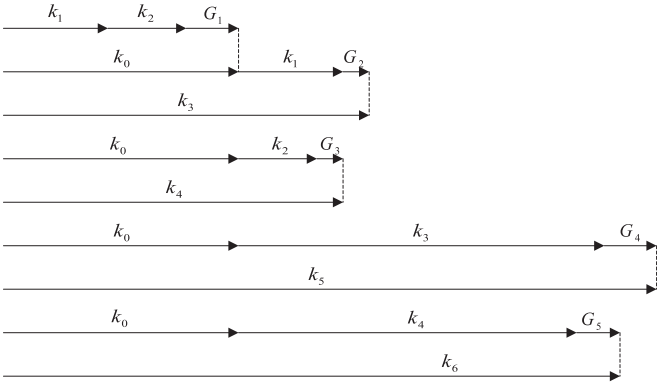

FIG. 4. The quasiphase-matching sketch of the cascaded nonlinear down-conversion and four sum-frequency processes. k_0,k_1,k_2,k_3,k_4,k_5, and k_6 are the wave vectors of pump ω_0 and the six generated beams $\omega_1,\omega_2,\omega_3,\omega_4,\omega_5$, and ω_6. G_1,G_2,G_3,G_4, and G_5 are five independent reciprocals provided by the OS to compensate the phase mismatching.

$$\tau\frac{d\bar{\alpha}_1}{dt} = -\frac{\gamma_1}{2}\bar{\alpha}_1 + \kappa_1\bar{\alpha}_0\bar{\alpha}_2^* - \kappa_2\bar{\alpha}_0^*\bar{\alpha}_3, \quad (14)$$

$$\tau\frac{d\bar{\alpha}_2}{dt} = -\frac{\gamma_2}{2}\bar{\alpha}_2 + \kappa_1\bar{\alpha}_0\bar{\alpha}_1^* - \kappa_3\bar{\alpha}_0^*\bar{\alpha}_4, \quad (15)$$

$$\tau\frac{d\bar{\alpha}_3}{dt} = -\frac{\gamma_3}{2}\bar{\alpha}_3 + \kappa_2\bar{\alpha}_0\bar{\alpha}_1 - \kappa_4\bar{\alpha}_0^*\bar{\alpha}_5, \quad (16)$$

$$\tau\frac{d\bar{\alpha}_4}{dt} = -\frac{\gamma_4}{2}\bar{\alpha}_4 + \kappa_3\bar{\alpha}_0\bar{\alpha}_2 - \kappa_5\bar{\alpha}_0^*\bar{\alpha}_6, \quad (17)$$

$$\tau\frac{d\bar{\alpha}_5}{dt} = -\frac{\gamma_5}{2}\bar{\alpha}_5 + \kappa_4\bar{\alpha}_0\bar{\alpha}_3, \quad (18)$$

$$\tau\frac{d\bar{\alpha}_6}{dt} = -\frac{\gamma_6}{2}\bar{\alpha}_6 + \kappa_5\bar{\alpha}_0\bar{\alpha}_4. \quad (19)$$

The equations can be solved by setting $\frac{d\bar{\alpha}_i}{dt} = 0$ ($i = 0,\ldots,6$) since, when time is long enough, mean values of the fields can be considered constant. Though the general analytical solution of the threshold and the mean value of the fields with different frequencies can be obtained, it is too complex. So we choose to obtain the threshold by a numerical method. For example, when $\gamma_0 = 0.01$, $\gamma_1 = 0.01$, $\gamma_2 = 0.01$, $\gamma_3 = 0.01$, $\gamma_4 = 0.01$, $\gamma_5 = 0.01$, $\gamma_6 = 0.01$, $\kappa_1 = 1.5\gamma_1$, $\kappa_2 = 1.5\gamma_1$, $\kappa_3 = 1.5\gamma_1$, $\kappa_4 = 1.5\gamma_1$, and $\kappa_5 = 1.5\gamma_1$, the threshold is $\epsilon_c = 0.584$.

After deriving the threshold for the pump value, we will investigate the entanglement characteristics of the six output fields both above and below the threshold. Since the mean values of the fields in the cavity are obtained, they can be used to linearize the classical motion equations for the fields in the cavity to obtain the equations of the fluctuations of the fields in the cavity:

$$\tau\frac{\partial}{\partial t}\delta\tilde{\alpha} = -M\delta\tilde{\alpha} + B\eta, \quad (20)$$

where

$$M = -\begin{bmatrix} M_1 & M_2 \\ M_2^* & M_1^* \end{bmatrix}, \tag{21}$$

$$M_1 = \begin{bmatrix} -\frac{\gamma_0}{2} & -\kappa_1\bar{\alpha}_2 & -\kappa_1\bar{\alpha}_1 & -\kappa_2\bar{\alpha}_1^* & -\kappa_3\bar{\alpha}_2^* & -\kappa_4\bar{\alpha}_3^* & -\kappa_5\bar{\alpha}_4^* \\ \kappa_1\bar{\alpha}_2^* & -\frac{\gamma_1}{2} & 0 & -\kappa_2\bar{\alpha}_0^* & 0 & 0 & 0 \\ \kappa_1\bar{\alpha}_1^* & 0 & -\frac{\gamma_2}{2} & 0 & -\kappa_3\bar{\alpha}_0^* & 0 & 0 \\ \kappa_2\bar{\alpha}_1 & \kappa_2\bar{\alpha}_0 & 0 & -\frac{\gamma_3}{2} & 0 & -\kappa_4\bar{\alpha}_0^* & 0 \\ \kappa_3\bar{\alpha}_2 & 0 & \kappa_3\bar{\alpha}_0 & 0 & -\frac{\gamma_4}{2} & 0 & -\kappa_5\bar{\alpha}_0^* \\ \kappa_4\bar{\alpha}_3 & 0 & 0 & \kappa_4\bar{\alpha}_0 & 0 & -\frac{\gamma_5}{2} & 0 \\ \kappa_5\bar{\alpha}_4 & 0 & 0 & 0 & \kappa_5\bar{\alpha}_0 & 0 & -\frac{\gamma_6}{2} \end{bmatrix}, \tag{22}$$

$$M_2 = \begin{bmatrix} 0 & -\kappa_2\bar{\alpha}_3 & -\kappa_3\bar{\alpha}_4 & -\kappa_4\bar{\alpha}_5 & -\kappa_5\bar{\alpha}_6 & 0 & 0 \\ -\kappa_2\bar{\alpha}_3 & 0 & \kappa_1\bar{\alpha}_0 & 0 & 0 & 0 & 0 \\ -\kappa_3\bar{\alpha}_4 & \kappa_1\bar{\alpha}_0 & 0 & 0 & 0 & 0 & 0 \\ -\kappa_4\bar{\alpha}_5 & 0 & 0 & 0 & 0 & 0 & 0 \\ -\kappa_5\bar{\alpha}_6 & 0 & 0 & 0 & 0 & 0 & 0 \\ 0 & 0 & 0 & 0 & 0 & 0 & 0 \\ 0 & 0 & 0 & 0 & 0 & 0 & 0 \end{bmatrix}. \tag{23}$$

The validity of linearization method requires that all the eigenvalues of matrix M have a positive real part [11]; these conditions are easily verified by the numerical method for the parameters which we use for calculation.

IV. SIX-PARTITE ENTANGLEMENT CHARACTERISTICS

Then we can obtain the spectral correlation matrix of the fields in the cavity in the frequency domain [18]:

$$S(\omega) = (M + i\omega\tau I)^{-1} B B^T (M^T - i\omega\tau I)^{-1}, \tag{24}$$

where ω is the analysis frequency and I is the identity matrix. The covariance elements of fields in the cavity can be obtained from matrix $S(\omega)$. Thus the covariance elements of the output fields can be obtained by applying boundary conditions [18,19]:

$$S^{\text{out}}_{X_i}(\omega) = 1 + 2\gamma_i S_{X_i}(\omega), \tag{25}$$

$$S^{\text{out}}_{X_i,X_J}(\omega) = 2\sqrt{\gamma_i\gamma_j} S_{X_i,X_j}(\omega), \tag{26}$$

where S_{X_i} are the variances of X_i and S_{X_i,X_j} are the covariances of X_i and X_j. The expressions for $\hat{Y}_i$ are similar to the equations above.

After deriving the covariance elements of the output fields, a sufficient inseparability criterion for CV multipartite entanglement is used to investigate the characteristics of the six-partite entanglement of the six generated beams both below and above the threshold [15]. The sufficient inseparability criterion for CV genuine six-partite entanglement consists of 15 inequalities. All of the partially separable forms have to be excluded to prove that the six modes are fully inseparable [15]. So at least five inequalities are needed to verify the full inseparability. In this work, we have chosen the following five inequalities to investigate the characteristics of the six-partite entanglement. When all of the following inequalities are violated, the six modes are fully inseparable.

$$S_{12} = \langle\delta^2(X_1 - X_2)\rangle + \langle\delta^2(Y_1 + Y_2 + g_3Y_3 + g_4Y_4 + g_5Y_5 + g_6Y_6)\rangle \geqslant 1, \tag{27}$$

$$S_{23} = \langle\delta^2(X_2 - X_3)\rangle + \langle\delta^2(g_1Y_1 + Y_2 + Y_3 + g_4Y_4 + g_5Y_5 + g_6Y_6)\rangle \geqslant 1, \tag{28}$$

$$S_{34} = \langle\delta^2(X_3 - X_4)\rangle + \langle\delta^2(g_1Y_1 + g_2Y_2 + Y_3 + Y_4 + g_5Y_5 + g_6Y_6)\rangle \geqslant 1, \tag{29}$$

$$S_{45} = \langle\delta^2(X_4 - X_5)\rangle + \langle\delta^2(g_1Y_1 + g_2Y_2 + g_3Y_3 + Y_4 + Y_5 + g_6Y_6)\rangle \geqslant 1, \tag{30}$$

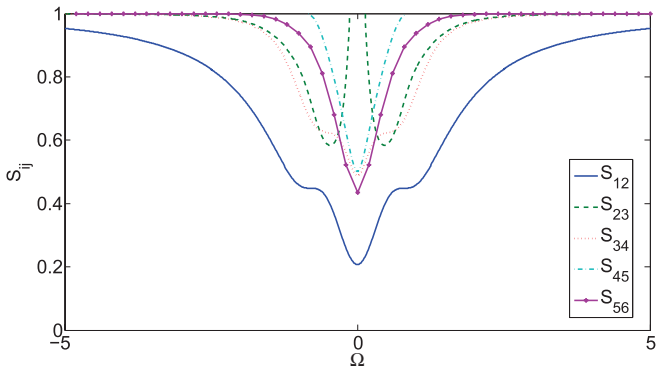

FIG. 5. (Color online) The quantum correlation spectra S_{ij} vs normalized frequency $\Omega = \omega\tau/\gamma_1$ for the six beams below the threshold.

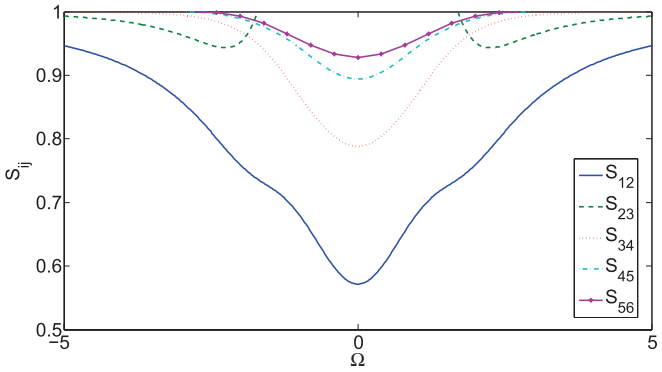

FIG. 6. (Color online) The quantum correlation spectra S_{ij} vs normalized frequency $\Omega = \omega\tau/\gamma_1$ for the six beams above the threshold.

$$S_{56} = \langle \delta^2(X_5 - X_6)\rangle + \langle \delta^2(g_1 Y_1 + g_2 Y_2 + g_3 Y_3 + g_4 Y_4 + Y_5 + Y_6)\rangle \geqslant 1. \quad (31)$$

In the inequalities above, S_{ij} $(i = 1,\ldots,6;\ j = 1,\ldots,6)$ represent the quantum correlation spectra of the output fields. $X_i = \frac{1}{2}(\hat{A}_i^{\text{out}} + \hat{A}_i^{\text{out}\dagger})$ and $Y_i = \frac{1}{2i}(\hat{A}_i^{\text{out}} - \hat{A}_i^{\text{out}\dagger})$ are the amplitude and phase quadrature operators of the output nonpump fields. g_i $(i = 1,\ldots,6)$ are arbitrary real scaling factors. The minimized value of the quantum correlation spectra can be obtained by choosing appropriate g_i. Although it is possible to derive analytical results of the quantum correlation spectra, they are too complex. To make the results more clear, we will show the results graphically. The entanglement characteristics are determined by the pump amplitude, nonlinear coefficients of nonlinear processes, and structure parameters of the superlattice. In addition, the

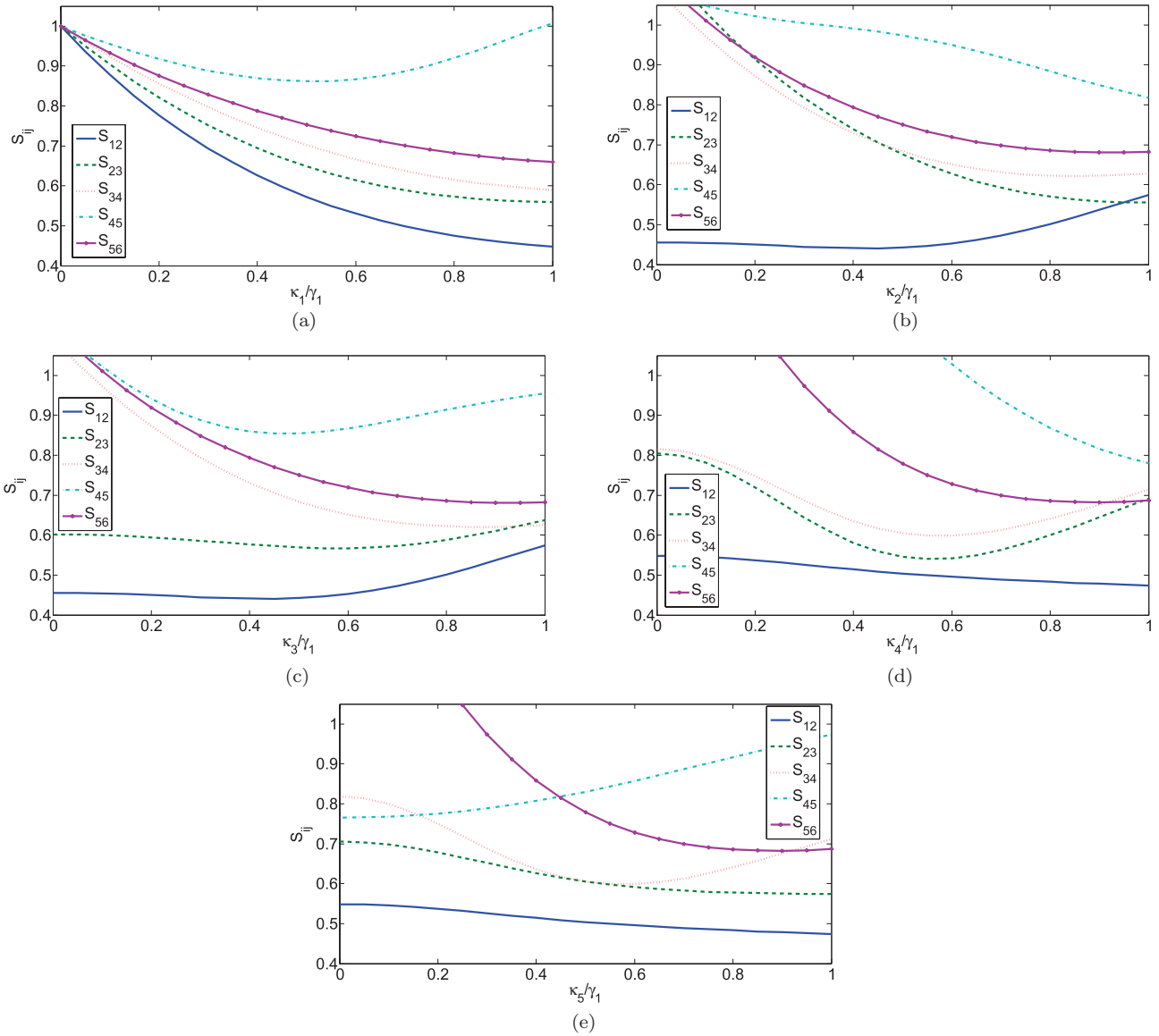

FIG. 7. (Color online) The quantum correlation spectra S_{ij} vs κ_i/γ_1. (a) The quantum correlation spectra S_{ij} vs κ_1/γ_1. (b) The quantum correlation spectra S_{ij} vs κ_2/γ_1. (c) The quantum correlation spectra S_{ij} vs κ_3/γ_1. (d) The quantum correlation spectra S_{ij} vs κ_4/γ_1. (e) The quantum correlation spectra S_{ij} vs κ_5/γ_1.

validity of the linearization method should also be verified when investigating the entanglement characteristics. So we will vary the parameters to investigate the entanglement both below and above the threshold. First, when $\gamma_0 = 0.01$, $\gamma_1 = 0.01$, $\gamma_2 = 0.01$, $\gamma_3 = 0.01$, $\gamma_4 = 0.01$, $\gamma_5 = 0.01$, $\gamma_6 = 0.01$, $\kappa_1 = 0.6\gamma_1$, $\kappa_2 = 0.6\gamma_1$, $\kappa_3 = 0.6\gamma_1$, $\kappa_4 = 0.6\gamma_1$, and $\kappa_5 = 0.6\gamma_1$, the entanglement characteristics among the six beams when the pump is below the threshold are shown in Fig. 5.

When the parameters are chosen as above, the quantum correlation spectra cannot be calculated when the pump value is above the threshold because the validity of the linearization method is not satisfied. So to investigate the entanglement characteristics above the threshold, the parameters should be chosen properly. For example, when $\gamma_0 = 0.01$, $\gamma_1 = 0.01$, $\gamma_2 = 0.01$, $\gamma_3 = 0.05$, $\gamma_4 = 0.05$, $\gamma_5 = 0.05$, $\gamma_6 = 0.05$, $\kappa_1 = 0.6\gamma_1$, $\kappa_2 = 0.6\gamma_1$, $\kappa_3 = 0.6\gamma_1$, $\kappa_4 = 0.6\gamma_1$, and $\kappa_5 = 0.6\gamma_1$, six-partite entanglement can be achieved above the threshold. When the pump amplitude is 2, which is above the threshold, $|\bar{\alpha}_0| = 0.444$, $|\bar{\alpha}_1| = 0.582$, $|\bar{\alpha}_2| = 0.582$, $|\bar{\alpha}_3| = 0.145$, $|\bar{\alpha}_4| = 0.145$, $|\bar{\alpha}_5| = 0.039$, and $|\bar{\alpha}_6| = 0.039$. The entanglement characteristics are shown in Fig. 6.

The values of the quantum correlation spectra are also influenced by κ_i/γ_1 $(i = 1, \ldots, 5)$ determined by pump amplitude, nonlinear coefficients of nonlinear processes, and structure parameters of the superlattice. We will show the results in Fig. 7. In Fig. 7, we plot the quantum correlation spectra S_{ij} versus κ_i/γ_1 with $\Omega = 0.6$, $\gamma_1 = 0.01$, $\gamma_2 = 0.01$, $\gamma_3 = 0.01$, $\gamma_4 = 0.01$, $\gamma_5 = 0.01$, $\gamma_6 = 0.01\kappa_1 = 0.75\gamma_1$, $\kappa_2 = 0.75\gamma_1$, $\kappa_3 = 0.75\gamma_1$, $\kappa_4 = 0.75\gamma_1$, $\kappa_5 = 0.75\gamma_1$, and the pump amplitude below the threshold. From Fig. 7(a), we can see that six-partite entanglement characteristics are influenced by the pump amplitude, and the best correlation spectra can be achieved near the threshold $\kappa_1/\gamma_1 = 0.876$. From Fig. 7(b), we can see that when $\kappa_2 = 0$, only S_{12} is below 1. It is because the sum frequency of the pump and the beam with frequency ω_1 does not occur; thus the beam with frequency ω_3 is not generated. When κ_2 is increasing, the energy of the pump and the beam with frequency ω_1 will be diverted to the beam with frequency ω_3, and S_{12} will increase, which indicates that the entanglement between the beams with frequencies ω_1 and ω_2 is weakened. From Fig. 7(c), we can see that when $\kappa_3 = 0$, only S_{12} and S_{23} are below 1. And as κ_3 increases, similar things happen to S_{12} and S_{23}. From Fig. 7(d), we can see that, when $\kappa_4 = 0$, only S_{12}, S_{23}, and S_{34} are below 1. And as κ_4 increases, S_{12} is not significantly influenced since the beam with frequency ω_1 and the beam with frequency ω_2 do not take part in the nonlinear process related to κ_4. A similar conclusion can be drawn from Fig. 7(e) as from Fig. 7(d).

To summarize, from Fig. 7, we draw the following conclusions. First, when energy is transferring from one mode to other modes, the entanglement characteristics will be influenced. Second, each coefficient can be adjusted to achieve the best entanglement characteristics. So the nonlinear coefficients can be optimized to achieve stronger entanglement for the six modes by designing the optical superlattice properly.

V. CONCLUSION

In this work, we theoretically investigated the generation of continuous-variable genuine six-partite entanglement using a nonlinear photonic crystal by a nonlinear parametric down-conversion cascaded with four sum-frequency processes. A possible structure of the crystal is also shown in this work. The results of our research show that when the parameters are chosen properly, six-partite entanglement can be achieved both below and above the threshold. And by choosing the proper pump amplitude and nonlinear coefficients, stronger entanglement can be obtained. So we think that more work can be done to improve the nonlinear coefficients of the nonlinear processes to reduce the quantum correlation spectra. Theoretically, this proposal can be extended to generate N-partite entanglement when we use a $N-2$ SFG and a PDC. However, as N increases, the nonlinear coupling coefficients of the nonlinear optical processes will decrease, so that entanglement among the N modes may not be generated successfully.

ACKNOWLEDGMENTS

We appreciate the inspiring discussion with Xin Tao. This work was supported by the National Natural Science Foundation of China (Grants No. 61102053, No. 61170228, No. 60970109, and No. 60801051), SJTU PRP (Grants No. T030PRP18001 and No. T030PRP19035), and the State Key Laboratory Foundation (Grant No. 2011GZKF031202).

[1] M. A. Nielsen and I. L. Chuang, *Quantum Computation and Quantum Information* (Cambridge University Press, Cambridge, 2000).

[2] P. G. Kwiat, K. Mattle, H. Weinfurter, A. Zeilinger, A. V. Sergienko, and Y. Shih, Phys. Rev. Lett. **75**, 4337 (1995).

[3] Y. H. Shih and C. O. Alley, Phys. Rev. Lett. **61**, 2921 (1988).

[4] S. L. Braunstein and P. van Loock, Rev. Mod. Phys. **77**, 513 (2005).

[5] T. Aoki, N. Takei, H. Yonezawa, K. Wakui, T. Hiraoka, A. Furusawa, and P. van Loock, Phys. Rev. Lett. **91**, 080404 (2003).

[6] P. van Loock and S. L. Braunstein, Phys. Rev. Lett. **87**, 247901 (2001).

[7] J. Zhang, C. Xie, and K. Peng, Phys. Rev. Lett. **95**, 170501 (2005).

[8] H. Yonezawa, T. Aoki, and A. Furusawa, Nature (London). **431**, 430 (2004).

[9] Y. B. Yu, Z. D. Xie, X. Q. Yu, H. X. Li, P. Xu, H. M. Yao, and S. N. Zhu, Phys. Rev. A **74**, 042332 (2006).

[10] H. T. Tan and G. X. Li, Phys. Rev. A **82**, 032322 (2010).

[11] H. Y. Leng, J. F. Wang, Y. B. Yu, X. Q. Yu, P. Xu, Z. D. Xie, J. S. Zhao, and S. N. Zhu, Phys. Rev. A **79**, 032337 (2009).

[12] A. S. Coelho, F. A. S. Barbosa, K. N. Cassemiro, A. S. Villar, M. Martinelli, and P. Nussenzveig, Science **326**, 823 (2009).

[13] M. Pysher, Y. Miwa, R. Shahrokhshahi, R. Bloomer, and O. Pfister, Phys. Rev. Lett. **107**, 030505 (2011).

[14] J. Jing, J. Zhang, Y. Yan, F. Zhao, C. Xie, and K. Peng, Phys. Rev. Lett. **90**, 167903 (2003).
[15] P. van Loock and A. Furusawa, Phys. Rev. A **67**, 052315 (2003).
[16] R. Lifshitz, A. Arie, and A. Bahabad, Phys. Rev. Lett. **95**, 133901 (2005).
[17] D. F. Walls and G. J. Milburn, *Quantum Optics* (Springer, Berlin, 1994).
[18] C. W. Gardiner, *Handbook of Stochastic Methods* (Springer, Berlin, 2002).
[19] M. J. Collett and C. W. Gardiner, Phys. Rev. A **30**, 1386 (1984).